A Monte Carlo study of water at an uncharged clay surface

A Monte Carlo study of water at an uncharged clay surface

C H Bridgeman†§ and N T Skipper‡

† Department of Chemistry, Lensfield Road, Cambridge CB2 1EW, UK
‡ Department of Physics, University College, Gower Street, London WCE1 6BT, UK

Abstract. Monte Carlo simulations have been used to study water confined between uncharged clay sheets. Low-energy sites for water at a talc surface were identified. The water molecules adsorbed onto these sites, which lie above the clay's hydroxyl group, are able to form strong hydrogen bonds with waters in the next hydration layer and so perturb the structure of this layer. No restructuring of the hydrogen bond network was apparent beyond this second layer.

1. Introduction

The influence of solid surfaces on the properties of liquid water is important in many situations. The behaviour of water at clay surfaces is of interest due to the geological and industrial importance of these minerals and as a means of investigating water–solid interfaces in general. Talc ($Mg_3Si_4O_{10}(OH)_2$) is an uncharged, trioctahedral 2:1 clay mineral whose surface consists of rings of SiO_4 tetrahedra. Hydroxyl groups belonging to the octahedral sheet lie at the centres of these rings. Measurement of the contact angle of water on talc indicates that a freshly cleaved surface is hydrophobic [1], although after outgassing at 523 K, talc displays an affinity towards water. This was interpreted as the adsorption of water through the growth of hydrogen-bonded clusters over the OH sites [2].

The behaviour of water adjacent to a variety of solid surfaces has been investigated both experimentally and via simulation. Lee and Rossky [3] performed MD simulations to investigate the structure and dynamics of water in contact with flat and structured hydrophobic surfaces and a hydroxylated silica surface (hydrophilic) and found, in all cases, structural perturbation of the solvent extending approximately 10 Å from the surface. These perturbations are strong only in the solvation layer. Water molecules adjacent to the hydrophilic surface were found to form three hydrogen bonds with the surface in a nearly ideal arrangement, while the hydrophobic surfaces caused water molecules to orientate with their dipole parallel to the surface and one hydrogen directed towards the surface and so excluded from forming hydrogen bonds. This is in agreement with a number of other MC and MD simulations using both rigid [4–6] and flexible [7] water models. The water diffusion coefficients for molecules adjacent to the hydrophobic surfaces were slightly increased parallel to and decreased perpendicular to the surface. The diffusion coefficients for water near the hydrophilic surface were decreased in all directions.

Monte Carlo simulation has been used to study water confined between mica [8] and smectite [9] layers. Using MC simulation, Delville [8] investigated the layered structure of water confined between charged and uncharged mica-like surfaces. Between the neutral

§ Author to whom any correspondence should be addressed.

mica-like sheets, two or three distinct and well ordered layers of water molecules were observed, depending on the separation of the sheets. Between the charged sheets at small interlayer spacings there exist two layers of water separated by a central layer of potassium counterions, while at larger spacings a third water layer becomes apparent but its concentration is less than that in the layers adjoining the mica, since the presence of the counterions partially excludes water from the central region. The adsorption of water vapour at the surfaces of clays has been studied via MC simulations [10]. The clays studied were kaolinite, a 1:1 clay, which has an OH saturated surface and a surface which contains only rings of SiO_4 tetrahedra and thus resembles the surface of talc, and uncharged potassium-mica which, in addition to silicon oxide, also contains aluminium oxide and potassium at its surface. In the case of kaolinite, the hydration layer at the talc-like surface is diffuse while the mica surface develops a dense liquid film with a maximum concentration 1.6 times that of liquid water.

The interaction of water with SiO_2 has been studied using NMR [11]. Resonance widths were measured and suggest long-range order of adsorbed water. The interaction forces between surfaces in liquids have received a great deal of attention ([12–14] for example). Long-range attractive forces have been observed between hydrophobic surfaces in water [15], while the forces between hydrophilic surfaces are short range and repulsive [16]. The structure of interlayer water in clays can be examined via neutron diffraction. This technique has been used to examine hydrated Na and Ni vermiculites [17]. The results of this study indicate that water molecules are oriented to form hydrogen bonds with the clay surface.

2. Computational method

The calculations described below were performed using the program *Monte* [18]. This program is designed to simulate molecular liquids between solid surfaces. Short-range interactions are treated using the minimum-image convention, and long-range Coulombic interactions are calculated using a Ewald sum.

Table 1. Charges for ions in the talc layer.

Species	Mg	Si	O ($z = 3.15$)	O ($z = 1.00$)	O(H)	(O)H
Charge (e)	2.00	1.20	-1.80	-1.00	-1.52	0.52

The program was used to study the behaviour of 256 TIP4P water molecules [19] confined between talc layers at a temperature of 300 K and a pressure of 1 atm. Simulations were performed in the constant-$N\sigma T$ ensemble, where σ is the pressure applied normal to the solid surface. This allows the distance between talc layers, i.e. the z-dimension of the unit cell, to adjust during the simulation. The ions in the talc layer were placed at the positions previously calculated from a total energy study [20], and the charges on these sites are given in table 1. The simulation cell consisted of a 4×8 array of talc unit cells parallel to the xy-plane centred at $z = 0$ and repeated at the top of the cell, $z = z_{max}$. The water molecules were placed between these two clay layers. The attempted translations and rotations for the interlayer molecules were chosen according to a Gaussian distribution, the width of which was adjusted during the course of the simulation to bring the acceptance rate for each type of move to 50%. After every five attempted water moves, the z-coordinate

was adjusted and the new configuration accepted with probability

$$p = \min\{1, \exp(-(\delta H/k_B T))\}. \tag{1}$$

Equilibration took 500 000 moves and was considered to have occurred when the average total energy and the z-coordinate had converged. The simulation was then continued for a further 2000 000 moves, during which average thermodynamic quantities and RDFs were calculated. Configurations were saved every 500 moves to allow detailed analysis later. The energy and layer separation of talc in the absence of water were also calculated.

3. Results and discussion

The average z-coordinate of the clay–water system was 30.30 ± 0.03 Å (cf. 9.182 ± 0.002 Å for dry talc) giving a volume change of 8157.6 Å^3 and a water density of 938 kg m^{-3} between the clay layers. The cohesive energy of the water between the clay layers was -41.31 ± 0.02 kJ mol^{-1} which is close to the energy of bulk TIP4P water (-42.27 ± 0.07 kJ mol^{-1} [21]), suggesting that the water structure is not greatly perturbed by the presence of the clay. The total energy of the talc–water system (per $Mg_3Si_4O_{10}(OH)_2$ structural unit) was -214.5 ± 0.1 kJ mol^{-1} and the energy of dry talc was 337.2 ± 0.1 kJ mol^{-1}. Hence the energy required to separate the clay layers is 109.26 kJ mol^{-1}, or 0.75 J m^2.
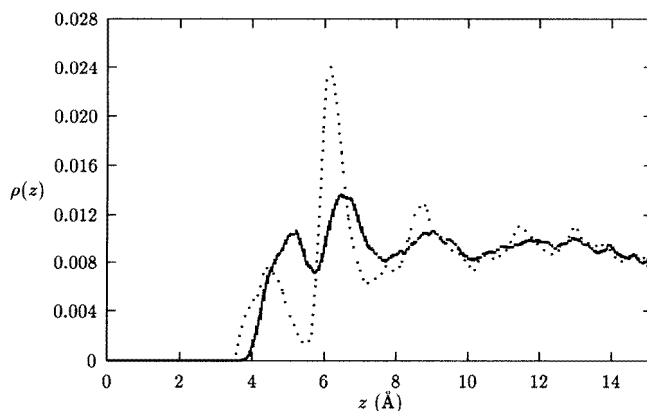
**Figure 1.** Density profiles for water oxygens (dotted line) and hydrogens (solid line).

The number density profile, $\rho(z)$, of water is shown in figure 1. The profile is calculated by considering the distance to the nearest clay layer and so is symmetric about the centre ($z = 15.15$ Å). Three layers of water are clearly distinguishable adjacent to the talc surface, after which the distribution becomes less structured. Water–water RDFs are presented in figure 2 averaged over the entire interlayer region and for water in the first three hydration layers. The first layer (0–5.45 Å) has a maximum at 2.85 Å and a second maximum of similar height and width at 5.25 Å. The presence of this second maximum, which is not present in the RDFs of subsequent layers, indicates structuring of the water imposed by the clay layer. Further examination of configurations saved during the simulation reveals that these waters are situated in the centre of the rings of SiO_4 tetrahedra, above the OH group. On average 72% of these sites are occupied and the average distance from the centre of the talc plane is 4.5 Å. No other sites are occupied by waters in this layer. Hence the peak at 5.25 Å is due to the water molecules occupying sites at the centre of neighbouring
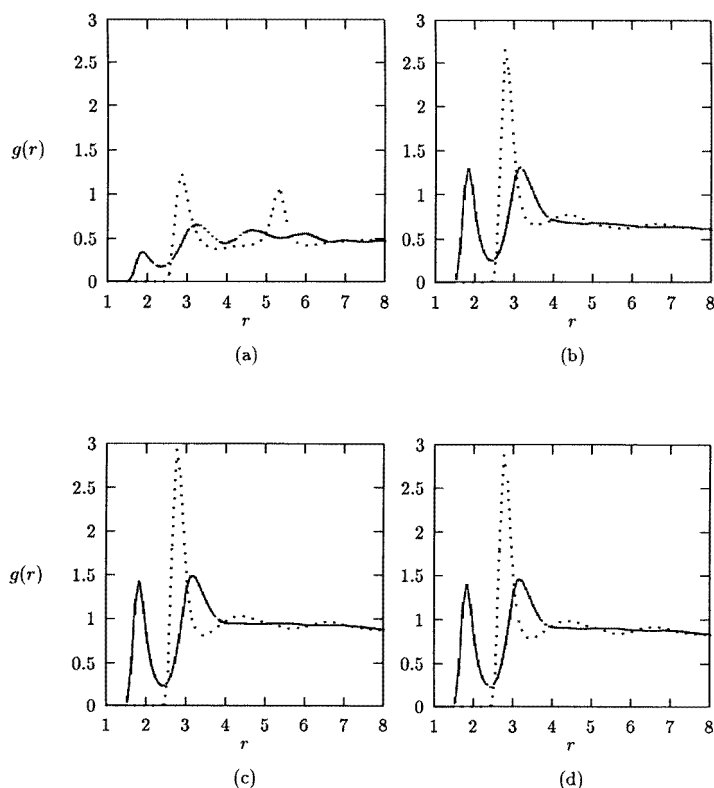
Figure 2. Radial distribution functions for waters in (a) the first hydration layer ($z = 0$–5.5 Å), (b) the second hydration layer ($z = 5.5$–7.5 Å), and (c) the third hydration layer ($z = 7.5$–10.5 Å), and (d) averaged over the entire interlayer region. Dotted lines represent g_{OO} and solid lines represent g_{OH}.

tetrahedral rings. RDFs for water in the second and third hydration layers are similar, showing little evidence of restructuring beyond the first layer. Figure 3 shows the water positions in the first three layers.

The angular probability distributions, $p(\theta)$, and angular probability density distributions, $\rho(\theta)$, for the first three hydration layers are plotted in figure 4. $p(\theta)$ is defined as the probability that a water molecule within the region under consideration (layer 1, 2 or 3) will have its dipole oriented at angle $\theta \pm \Delta\theta/2$ to the z-axis. $\rho(\theta)$ takes into account the element of area associated with each angle and is found by calculating $p(\theta)/\sin(\theta)$. $p(\theta)$ and $\rho(\theta)$ are normalized so that the area under each curve is unity. The dipole orientation in the first layer is notably different to that in subsequent layers. The probability distribution is approximately gaussian and centred around an angle of 45°. This is consistent with the results of a total energy study of hydrated talc [20], where the minimum-energy configuration was with the water molecule lying parallel to and midway between the talc sheets (i.e. 4.9 Å from the centre of each sheet) and a second configuration only 21.3 kJ mol^{-1} higher had the water 4 Å from the centre of the lower clay sheet and the dipole directed along the z-axis. In the second and third hydration layers, $p(\theta)$ is centred around an angle of 90° indicating that the dipole is as likely to be directed towards the layer as away from it. By the third layer, $\rho(\theta)$ is approximately equal at all angles indicating a random distribution.
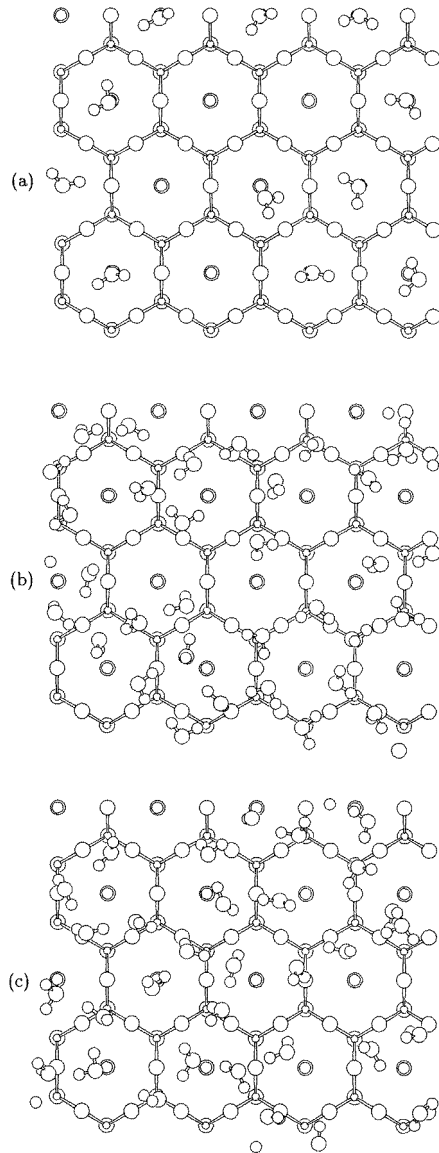
Figure 3. Positions of the water molecules above the talc surface, (a) $z = 0$–5.5 Å, (b) $z = 5.5$–7.5 Å, (c) $z = 7.5$–10.5 Å.

The average binding energy of a water molecule as a function of its distance from the centre of the clay layer was calculated according to the equation

$$U_r = \frac{1}{N_r} \sum_{i=1}^{N_r} \sum_{j=1}^{N_{cut}} U(r_{ij}) \tag{2}$$

where N_r is defined as the number of water molecules between z and $z + \delta z$, N_{cut} is the number of water molecules within a chosen cut-off distance, r_{cut}, of molecule i, and $U(r_{ij})$ is the interaction energy of molecules i and j. The cut-off distance was chosen to be 9 Å
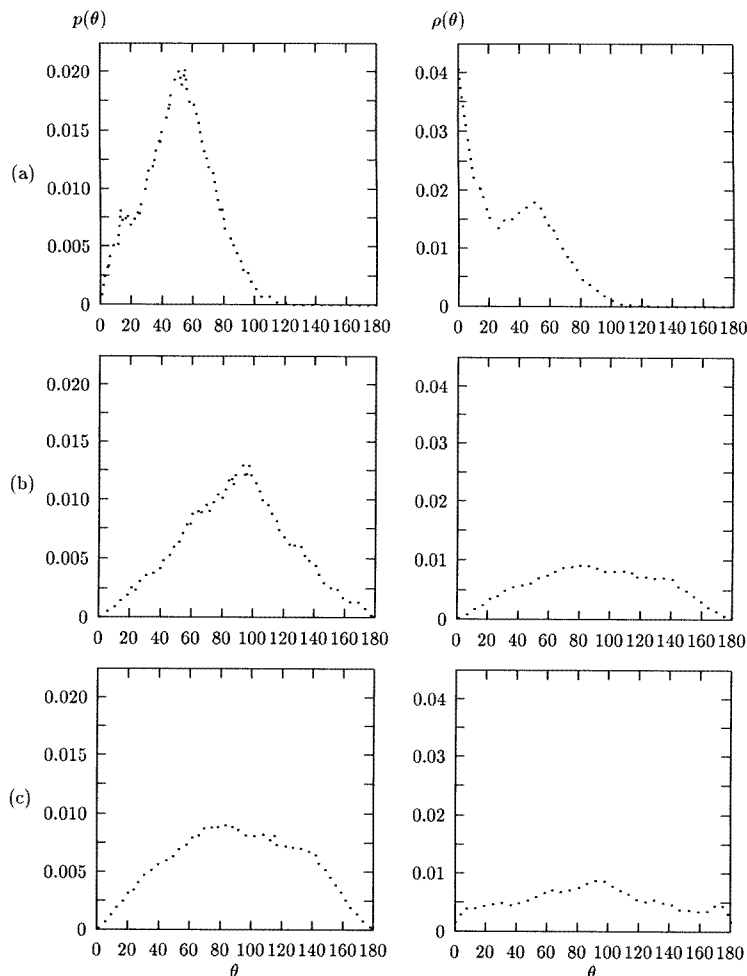
Figure 4. Probability $p(\theta)$ and probability density $\rho(\theta)$ distributions for the angle between the water dipole and the z-axis in the first (a), second (b) and third (c) hydration layers.

which is slightly less than half the minimum cell dimension, and only one simulation cell need be included in the summation. The average total binding energy per water molecule is plotted in figure 5. The binding energy due to interactions with other waters and with the talc layer are also shown. Beyond the first hydration layer the energy of interaction with the talc is approximately zero and so any modification in the intermolecular structure of the water molecules in the second hydration layer must be due principally to their interaction with those in the first hydration layer.

The dipole distributions and the similarity between the RDFs for the second and third hydration layers suggests minimal restructuring of the water beyond the first hydration layer. However, the binding energy is maximum for water in the second hydration layer suggesting a maximization of hydrogen bonding for these molecules. Examination of the $O \cdots H$ distance and the $O-H \cdots O$ angle for nearest-neighbour water molecules revealed that those in the second hydration layer form shorter, straighter bonds with those in the first layer (2.5 ± 0.1 Å, $135°$) than with waters in their own or higher layers (2.7 ± 0.2 Å, $122°$).

$E(z)$ (kJ mol^{-1})
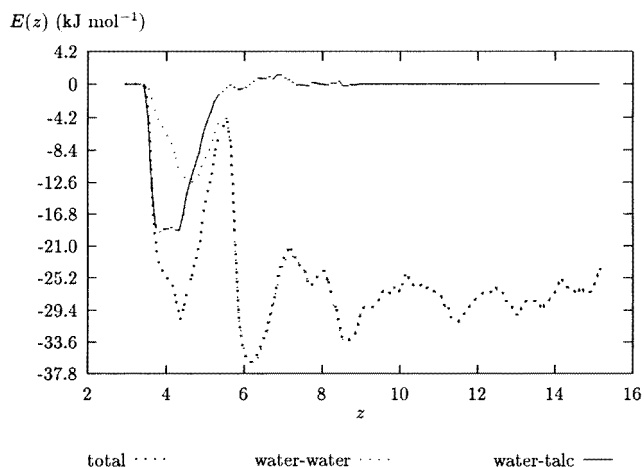
Figure 5. The binding energy per water molecule at a distance z from the centre of the talc layer.

4. Conclusion

Monte Carlo simulations were used to study water confined between uncharged clay sheets. Low-energy sites for water at a talc surface were identified. These are situated above the clay's hydroxyl groups and can each accommodate a single water molecule, thus allowing the formation of a diffuse layer of water at the surface of the clay. These water molecules form strong hydrogen bonds with the adjacent layer of water molecules and so perturb the structure of this layer. No restructuring of the hydrogen bond network was apparent beyond this second layer.

References

[1] Schrader M E and Yariv S 1990 *J. Colloid Interface Sci.* **136** 85–94
[2] Michot L J, Villiéras F, François M, Yvon J, LeDred R and Cases J M 1994 *Langmuir* **10** 3765–73
[3] Lee S-H and Rossky P J 1994 *J. Chem. Phys.* **100** 3334–45
[4] Jönsson B 1981 *Chem. Phys. Lett.* **82** 520–5
[5] Sonnenschein R and Heinzinger K 1983 *Chem. Phys. Lett.* **102** 550–4
[6] Barabino G, Gavotti C and Marchesi M 1984 *Chem. Phys. Lett.* **104** 478–84
[7] Zhu S-B and Robinson G W 1991 *J. Chem. Phys.* **94** 1403–10
[8] Delville A 1993 *J. Phys. Chem.* **97** 9703–12
[9] Skipper N T, Refson K and McConnell J D C 1991 *J. Chem. Phys.* **94** 7434–45
[10] Delville A 1995 *J. Phys. Chem.* **99** 2033–7
[11] Sermon P A 1980 *J. Chem. Soc. Faraday Trans.* I **76** 885–8
[12] Cowley A C, Fuller N L, Rand R P and Parsegian V A 1978 *Biochemistry* **17** 3163–8
[13] Christenson H K and Horn R G 1983 *Chem. Phys. Lett.* **98** 45–8
[14] Tsao Y-H and Evans D F 1993 *Langmuir* **9** 779–85
[15] Israelachvili J and Pashley R 1982 *Nature* **300** 341–2
[16] Israelachvili J and Pashley R 1983 *Nature* **306** 249–50
[17] Skipper N T, Soper A K and McConnell J D C 1991 *J. Chem. Phys.* **94** 5751–60
[18] Skipper N T 1992 *Monte* University College, London
[19] Jorgensen W L, Chandrasekhar J and Madura J D 1983 *J. Chem. Phys.* **79** 926–35
[20] Bridgeman C H, Buckingham A D, Skipper N T and Payne M C 1996 *Mol. Phys* **89** 879–88
[21] Jorgensen W L and Madura J D 1985 *Mol. Phys* **56** 1381–92